I-1. PROJECT RESEARCHES

Project 1

PR1 Improvement of Characterization Techniques in High-Energy-Particle Irradiation Research

A. Kinomura

Institute for Integrated Radiation and Nuclear Science, Kyoto University

OBJECTIVES: Irradiation facilities of high-energy particles for neutrons (Material Controlled irradiation Facility), ions (e.g., Heavy ion irradiation facility) and electrons (Temperature-controlled irradiation facilities, KUR-LINAC) have been extensively developed at the Institute for Integrated Radiation and Nuclear Science. The developed facilities have been in operation and opened for joint research projects. One of the objectives of this project is to further improve or optimize irradiation facilities for advanced irradiation experiments.

As characterization techniques for irradiated materials, a slow positron-beam system and a focused ion beam system have been developed and introduced, respectively, in addition to previous characterization facilities such as an electron microscope, an electron-spin-resonance spectrometer, a bulk positron annihilation spectrometer and a thermal desorption spectrometer. Another objective is to introduce new techniques or reconsider analytical methods of previously used characterization techniques.

Based on these two objectives, we expect the enhancement of previous studies and the attraction of new users for the joint research program.

The allotted research subject (ARS) and individual co-researchers are listed below. Note that the titles of research subjects are based on individual reports.

ARS-1:
Study on efficient use of positron moderation materials (A. Kinomura *et al.*)

ARS-2:
Temperature dependence of electron-irradiation effects on diffusion coefficient of Cu in Fe studied by atom probe tomography (K. Inoue *et al.*)

ARS-3:
Change in positron annihilation lifetime of vacancies by hydrogen charging in tungsten 2 (K. Sato *et al.*)

ARS-4:
Electron paramagnetic resonance study on gamma-ray irradiated ZnO bulk single crystal (K. Kuriyama *et al.*)

ARS-5:
The first challenging study on corrosion resistance of fusion divertor materials to liquid metal during electron irradiation (M. Akiyoshi *et al.*)

ARS-6:
Positron annihilation study of Fe-Cr binary alloy after electron irradiation (T. Onitsuka *et al.*)

ARS-7:
PAS study on free volume in several diamond-like carbon thin films (K. Kanda *et al.*)

ARS-8
Positron annihilation spectroscopy on diamond-like carbon films (S. Nakao *et al.*)

RESULTS: In ARS-1, the brightness enhancement system of the KUR slow positron system was evaluated with a positron beam. A total enhancement of the brightness was estimated to be approximately 4. The efficiency of the remoderator was measured to be approximately 2%

In ARS-2, Electron-irradiation was performed for Fe-1.0wt.%Cu alloy with an 8 MeV electron beam at 310 - 475 °C. Needle-like samples for atom probe tomography (APT) were fabricated and diffusivity Cu in Fe was successfully determined by APT measurements.

In ARS-3, high purity tungsten irradiated by 8 MeV electrons were characterized by positron lifetime spectroscopy to investigate the effect of hydrogen charging in vacancies. For comparison, first-principle calculations for atomic position and density for valence electrons were carried using the Vienna Ab initio Simulation Package (VASP) code.

In ARS-4, electron paramagnetic resonance (EPR) measurements were performed for single-crystalline ZnO samples by Co-60 gamma-ray irradiation to introduce vacancies. Red light illumination at 77 K significantly changed the EPR spactra showing the change of ionization states by light illumination.

In ARS-5, aluminum rich ferritic steel (Fe-18Cr-3.3Al-0.4Si) NTK04L with 100μm Al_2O_3 oxidization coating was enclosed with tin in a newly developed irradiation container. The validity of ceramic coating under irradiation environment using KURNS-LINAC was verified.

In ARS-6, electron irradiation by KURRI-LINAC for Fe-40Cr alloy samples were performed at elevated temperatures to investigate phase decomposition under irradiation.

In ARS-7, The change of free volume in hydrogenated DLC film by the irradiation of soft x-rays were characterized by positron annihilation spectroscopy using the slow positron beam system (B-1) at KUR. The S value of hydrogenated DLC film was lowered by the soft x-ray irradiation.

In ARS-8, several types of DLC and carbon films deposited by plasma-based ion implantation under different conditions were characterized by Doppler broadening measurements using the KUR slow positron beam system. Resutls suggest that the situation of the defect in the type III-VI films may be similar in the case of as-grown films.

SUMMARY: In addition to developments on the slow positron beamline and a sample holder for electron irradiation, combinations of new materials and different irradiation/characterization techniques were continuously performed in the line of the objectives of this project. Such studies may enhance new concepts and techniques in the future.

PR1-1 **Study on Efficient Use of Positron Moderation Materials**

A. Kinomura, N. Oshima[1], Y. Kuzuya and A. Yabuuchi

Institute for Integrated Radiation and Nuclear Science, Kyoto University
[1]National Institute of Advanced Industrial Science and Technology (AIST)

INTRODUCTION: Positron annihilation spectroscopy is a unique analytical method to detect vacancy-type defects and free volume of materials. Energy-variable mono-energetic positron beams (slow positron beams) are important to perform depth-dependent positron annihilation spectroscopy of thin films or surface layers. Intense positron sources are required to efficiently obtain slow positron beams. In general, positron sources based on pair creation have higher intensity than radioisotope-based positron sources. Therefore, positron sources using pair-creation by gamma-rays from a nuclear reactor have been developed by using Kyoto University research Reactor (KUR). In the case of the KUR, the source size of the KUR slow positron beam is approximately 30 mm in diameter. For typical sample sizes of materials analysis ($\leq$10 mm), it is necessary to reduce beam sizes efficiently while keeping beam intensity as high as possible. For this purpose, brightness enhancement techniques are used. In this study, we have evaluated the brightness enhancement system in the KUR slow positron beam system.

EXPERIMENTS: The brightness enhancement system of the KUR slow positron beam system has been examined using positron beams after the KUR operation was restarted in August 2017. A single-crystalline Ni thin film was used as a remoderator of the brightness enhancement system. The Ni remoderator film was annealed in the quartz tube furnace before installation and cleaned by thermally excited hydrogen atoms after installation.

A series of experiments were performed for the brightness enhancement system: (1) Optimization of bias-voltages and solenoid/Helmholtz coil currents to maximize positron-beam intensities. (2) Adjustment of a focusing lens of the brightness enhancement system with a microchannel plate (MCP). (3) Transport of a brightness-enhanced beam to the downstream direction. (4) Efficiency evaluation of remoderator thin films before and after the brightness enhancement system.

RESULTS: The trajectory and intensity of the beam were optimized by adjusting voltages for the source components and currents for transport and steering coils by observing the phosphor-screen images on the microchannel plates (MCP's). The excitation current of the focusing lens of the brightness enhancement system was optimized by observing the spot images on the microchannel plate positioned at the focal point of the lens. The brightness-enhanced beam was transported to the sample chamber and the final spot sized was evaluated by using the MCP positioned at the sample position. Spot sizes for horizontal and vertical directions were slightly different. A spot area was reduced by a factor of approximately 20 after focusing at the brightness enhancement system. The efficiency of the remoderator was measured to be ~2% by gamma-ray intensities from the MCPs placed before and after the brightness enhancement system. A total ehancement of the brightness was estimated to be approximately 4.

The brightness-enhanced beam was transported through a pulsing system with a transmission-type chopper. Energy distribution of the positron beam can be evaluated by changing chopper bias voltage. Fig. 1 shows the energy distributions measured by using the chopper electrode of the pulsing system. Figs. 1(a) and 1(b) correspond to the energy distribution before and after the brightness enhancement, respectively. In the case of Fig. 1(a), the focusing lens was turned off and the Ni moderator was retracted from the center of the brightness enhancement system. Different extraction voltages were applied to W moderator electrodes at the positron source of the beamline. Two peaks were identified with a width of 10 – 14 eV in Fig. 1(a). In the case of Fig. 1(b) with the brightness enhanced beam, one narrow peak with a width below 3 eV was obtained. Apparently the energy distribution was reduced after the brightness enhancement. It can be an important advantage for beam pulsing.

In summary, the brightness enhancement system of the KUR slow positron system was evaluated with a positron beam during the KUR operation. The energy distribution of the beam was significantly reduced after the brightness enhancement. Further optimization of the system is in progress.

REFERENCE:

[1] Y. Kuzuya *et al.* J. Phys. Conf. Series **791** (2017) 012012.

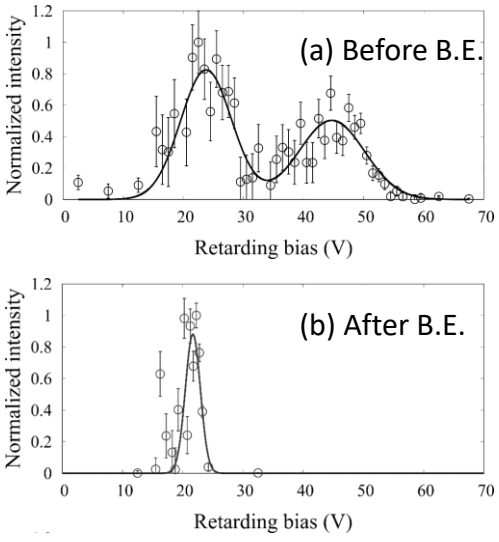

Fig. 1. Energy distribution of the positron beams before and after brightness enhancement (B.E.).

PR1-2 Temperature dependence of electron-irradiation effects on diffusion coefficient of Cu in Fe studied by atom probe tomography

T. Toyama, K. Inoue, Y. Nagai, Y. Shimizu, K. Yoshida, C. Zhao, S. Lan, T. Onitsuka[1], A. Kimomura[2], T. Yoshiie[2], Q. Xu[2], A. Yabuuchi[2]

Institute for Materials Research, Tohoku University

[1]Research Institute of Nuclear Engineering, Fukui University

[2]KURNS, Kyoto University

INTRODUCTION: A reactor pressure vessel (RPV) in a nuclear power plant is thick steel container that holds nuclear fuels, control rods and primary cooling water. The safety of RPV must be guaranteed. Therefore, irradiation-induced embrittlement of RPV steels is vital issue for the safe operation of nuclear power plants. One of the main origins for the irradiation-induced embrittlement of RPV is nano-sized Cu precipitates formed by neutron-irradiation. The diffusion coefficient, *D*, of Cu in Fe is the important basic quantities to understand the kinetics of Cu precipitation [1, 2].

Cu diffusion in Fe occurs by vacancy mechanism and is affected by the concentration of the vacancies in the material. Therefore, Cu diffusivity can be enhanced by irradiation because the vacancies and interstitials are remarkably induced during irradiation. In order to study the electron-irradiation effects on Cu diffusivity in Fe, we employ the electron irradiation at KUR LINAC which can induce simple Frenkel pairs. In the previous study, we investigated Cu diffusion coefficient under electron irradiation at 475℃ in Fe-1.0wt.%Cu alloys via precipitation kinetics using atom probe tomography (APT). The irradiation enhanced Cu diffusivity was clearly observed. In this study, we proceed to investigate Cu diffusion coefficient under electron irradiation in Fe-1.0wt.%Cu alloys at different temperature to reveal the temperature dependency of Cu diffusion coefficient for further understanding of the electron-irradiation effects on Cu diffusion coefficient.

EXPERIMENTS: Fe-1.0wt.%Cu alloy was made from high-purity (5N) Fe and Cu. A plate of 5 mm × 5 mm × 1 mm was fabricated and the surface of the sample was mechanically polished with abrasive papers of #2000. After removal of the machined layer by chemical polishing, the sample was annealed at 825℃ for 4 hours followed by quenching into ice-water.

Electron-irradiation was performed with electron beam with energy of 8 MeV at KUR LINAC. The irradiation dose rates, irradiation temperature, and irradiation time were 4.5 - 6.5×10^{-9} dpa/s, 310 - 475℃, and 1 - 2 hours respectively.

After electron-irradiation, needle-like samples for APT were fabricated with focused-ion beam apparatus. In APT measurement, a voltage pulse mode was employed at temperature of 50 K, pulse fraction of 20%, and a repetition frequency of 200 kHz.

RESULTS: Figure 1 shows atom map of Cu in the electron-irradiated Fe-Cu alloy at various irradiation conditions. Cu precipitates were clearly observed. The number density and the average size of Cu precipitates were analyzed with the standard analysis method. The Cu concentration in Fe matrix was also analyzed. With these parameters, the diffusion coefficient of Cu was estimated by using a formula concerning the diffusion coefficient and precipitation kinetics [3]. Figure 2 shows the Arrhenius plot of the *D* of Cu in Fe in the studied sample together with the *D* under thermal-aged samples [1]. The *D* under electron irradiation obtained in this study was much higher than that in thermal-aged condition. The *D* under electron irradiation was almost constant in the temperature range investigated in this study and was increased with increasing the dose rate. By comparing with estimation of vacancy concentration under irradiation by rate equation model, it is suggested that the observed enhancement of Cu diffusion is quantitatively attributed to the enhancement of vacancy concentration due to electron irradiation.

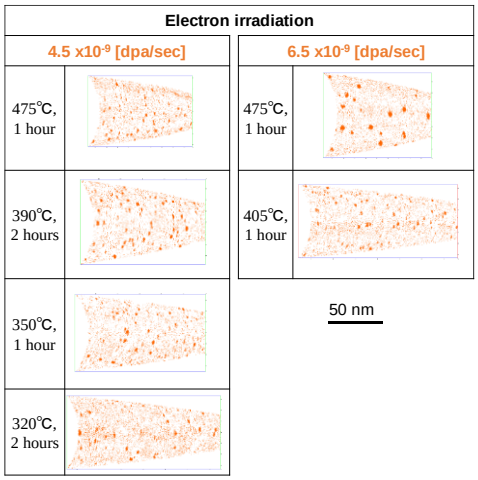

Figure 1: Atom maps of Cu in the electron-irradiated Fe-1.0wt. %Cu alloy at various irradiation conditions.

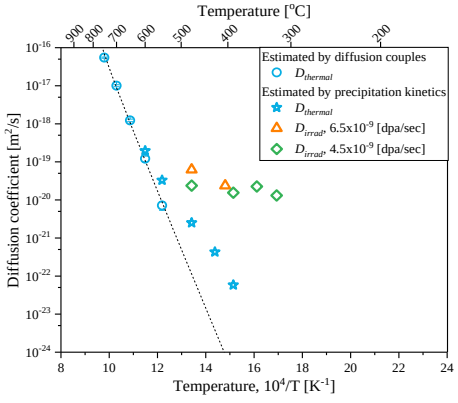

Figure 2: Arrhenius plot of the diffusion coefficient of Cu in Fe.

REFERENCES:

[1] T. Toyama *et al.*, Scrip. Mater., **83** (2014) 5-8.

[2] M. Shimodaira *et al.*, Mater. Trans., **9** (2015) 1513-1516.

[3] M. Koiwa and H. Nakajima, Diffusion in materials (Uchidarokakuho, 2009).

PR1-3 Change in Positron Annihilation Lifetime of Vacancies by Hydrogen Charging in Tungsten 2

K. Sato, Y. Kondo, M. Ota, Q. Xu[1], A. Yabuuchi[1], A. Kinomura[1]

Graduate School of Science and Engineering, Kagoshima University

[1]*KURNS, Kyoto University*

INTRODUCTION: The study of defect-hydrogen isotope complexes is an important issue for the structural materials of fusion reactor. In fusion reactor, neutrons introduce not only a variety of defects but also hydrogen and helium atoms formed by nuclear reaction of (n,p) and (n,α), respectively. In plasma-facing materials (PFMs), hydrogen isotopes penetrate by exposure to fusion plasma. The hydrogen isotopes interact with the irradiation-induced defects, and remain in the materials [1−3]. Retention of hydrogen isotopes leads to a decrease in mechanical properties of materials, e.g. hydrogen embrittlement etc. Tungsten is one of strong candidates for PFMs, which have high melting point, high thermal conductivity, and low sputtering erosion. However, hydrogen solubility is quite low, and interaction between hydrogen atoms and defects is strong [4]. Therefore, to study the interaction between hydrogen and defects is especially important in tungsten. In this study, we calculated the positron annihilation lifetime (PAL) of vacancies containing hydrogen atoms.

EXPERIMENTS: The Schrödinger equation for positron wave function was solved in the method developed by Puska and Nieminen [5]. In this calculation, the potential for a positron, which consisted of a Coulomb potential from nuclei and electrons and a correlation potential between a positron and an electron, must be given. To obtain the Coulomb potential from electrons, electron density was required, which was constructed by superposition of the atomic wave function given by Herman and Skillman [6] for core electrons (1s, 2s, 2p, 3s, 3p, 3d, 4s, 4p, 4d, 4f, 5s, 5p) and was obtained by the first-principle calculation for valence electrons (5d, 6s) (see next paragraph). The correlation potential was given by Boronski and Nieminen [7] based on the local density approximation. The numerical method developed by Kimball and Shortley [8] was used to solve the Schrödinger equation. Enhancement factors arising from the positron-electron correlation effects developed by Boronski and Nieminen [7,9] were used. Atomic position was also determined by the first-principle calculation.

The first-principle calculations for atomic position and density for valence electrons were carried out using the Vienna *Ab initio* Simulation Package (VASP) code [10,11] with projected augment wave (PAW) potentials [12]. The generalized gradient approximation (GGA) developed by Perdew, Burke and Ernzerhof (PBE) [13] was applied for the exchange-correlation energy functional. Lattice cell size was 128 atoms (4 × 4 × 4× 2), and 3 × 3 × 3 **k**-point grid of Monkhorst-Pack scheme [14] were used. The plane-wave energy cutoff was 325 eV. Ionic relaxation was performed until the force acting on every atom became smaller than 0.005 eV/Å. For the PAL calculation, cell shape (cubic) was fixed in this study. Lattice constant of 3.1695 Å was used, which obtained by the cell volume relaxation of perfect lattice.

RESULTS: Positron density heightens at vacancy site, and lowers by the existence of hydrogen atoms. The hydrogen atoms exist on the inner surface of the vacancy, and shifts from Octahedral site as reported by Ohsawa *et al*. [4,15] The simulated PAL of single vacancies containing one, two, three, four, five and six hydrogen atoms was 199 ps, 185 ps, 170 ps, 162 ps, 153 ps, 145 ps and 142 ps, respectively. The PAL of single vacancies containing no hydrogen (199 ps) is almost the same as the previous study (200 ps) [16]. When first hydrogen atom is added to a vacancy, the decrease of the PAL is approximately 15 ps. When second hydrogen atom is added to a vacancy-one hydrogen complex, it is also approximately 15 ps. When third, fourth, and fifth hydrogen atom is added to a vacancy-hydrogens complex, it is approximately 10 ps. When sixth hydrogen atom is added, it is a few pico-seconds. The trend of the change in the PAL is the same as the previous study [16], however, the decrease of the PAL is smaller in this study. This is caused by the location of first hydrogen atom added to single vacancy. The decrease of the PAL after hydrogen charging was approximately 20 ps in experiments. From simulation, when first and second hydrogen atom was added to vacancies, the decrease of the PAL is approximately 15 ps, respectively. It is expected that one vacancy captures one or two hydrogen atoms (on average 1.5 atoms).

REFERENCES:

[1] N. Yoshida, J. Nucl. Mater. **266-269** (1999) 197.
[2] M. Tokitani *et al.*, J. Nucl. Mater. **363** (2007) 443.
[3] V.Kh. Alimov *et al.*, J. Nucl. Mater. **375** (2008) 192.
[4] K. Ohsawa *et al.*, Phys. Rev. B **82** (2010) 184117.
[5] M.J. Puska and R.M. Nieminen, J. Phys. F **13** (1983) 333.
[6] F. Herman and S. Skillman, Atomic Structure Calculations, Prentice Hall, Inc. (1963).
[7] E. Boronski and R.M. Nieminen, Phys. Rev. B **34** (1986) 3829.
[8] G.E. Kimball and G.H. Shortley, Phys. Rev. **45** (1934) 815.
[9] M.J. Puska *et al.*, Phys. Rev. B **52** (1995) 10947.
[10] G. Kresse and J. Hafner, Phys. Rev. B **47** (1993) 558.
[11] G. Kresse and J. Furthmüller, Phys. Rev. B **54** (1996) 11169.
[12] P.E. Blöchl, Phys. Rev. B **50** (1994) 17953.
[13] J.P. Perdew *et al.,* Phys. Rev. Lett. **77** (1996) 3865.
[14] H.J. Monkhorst and J.D. Pack, Phys. Rev. B **13** (1976) 5188.
[15] K. Ohsawa *et al.*, Phys. Rev. B **85** (2012) 094102.
[16] T. Troev *et al.,* Nucl. Inst. Meth. Phys. Res. B **267** (2009) 535.

PR1-4 Electron paramagnetic resonance study on gamma-ray irradiated ZnO bulk single crystal

K. Kuriyama, T. Nishimura, K. Sato, J. Tashiro,
K. Kushida[1], A. Yabuuchi[2], Q. Xu[2] and A. Kinomura[2]

College of Engineering and Research Center of Ion Beam Technology, Hosei University

[1]*Osaka Kyoiku University*

[2] *Institute for Integrated Radiation and Nuclear Science, Kyoto University*

INTRODUCTION: Examining the defects caused by various radiations to ZnO and GaN by assuming the space environment is important. It is expected that the radiation damage is induced by Compton electrons emitted by the high dose gamma-ray irradiation. In our previous study, we reported the modification of the yellow luminescence in GaN bulk single crystal by gamma-ray irradiation [1]. The resistivity varies from 30 Ωcm for an un-irradiated sample to 10^4 Ωcm for gamma-ray irradiated one. The high resistivity was attributed to the carrier compensation due to the deep acceptor level relating to interstitial nitrogen atoms. We also reported that the persistent photoconductivity by electron-irradiated ZnO [2] and a shallow donor level relating to hydrogen interstitial by H-ion implanted ZnO [3]. In the present study, we report the existence of oxygen vacancy in gamma-ray irradiated ZnO by the electron paramagnetic resonance (EPR).

EXPERIMENTS: ZnO bulk single crystals with a thickness of 500 μm were used. The crystals were irradiated at room temperature with gamma-rays of 1.17 and 1.33 MeV from a cobalt-60 source of Institute for Integrated Radiation and Nuclear Science, Kyoto University. Samples were irradiated with an absorp-tion dose rate of 1.771 KGy/h. Total gamma-ray dose was 170 kGy. The resistivity varied from 4.1 x 10^4 Ωcm for an un-irradiated sample to 3.1 x 10^2 Ωcm for gamma-ray irradiated one. The EPR signal was meas-ured at 77 K.

RESULTS: Figure 1 shows EPR spectra in gamma-ray irradiated ZnO. A signal with g =1.996 was assigned to the oxygen vacancy of + charge state (V_O^+) observed in electron-irradiated ZnO [2]. This signal observed under no illumination disappeared after 10-min illumination of a red LED (λ=654 nm; 1.96 eV) at 77 K. The oxygen vacancy of V_O^+ states exists at about 1 eV below the conduction band. By the red LED illumination, electrons excited from the V_O^+ state are captured by V_O^{2+} as the defect localized state [4] in the conduction band. Therefore, V_O^+ states disappear. Since V_O^+ states behave as a deep donor (900~1200 meV), they are not an origin of low resistivity. In analogy with the low resistivity after Al-implanted ZnO [5], the decrease in resistivity after gamma-ray irradiation would be attributed to the shallow donor (30 meV below the conduction band [6]) due to interstitial zinc atoms.

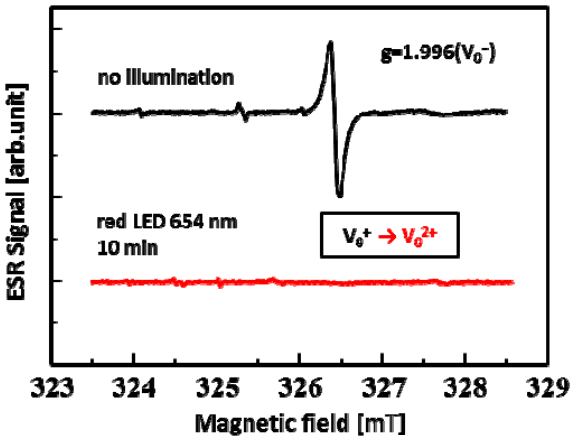

Fig.1 Electron paramagnetic resonance (EPR) spectra at 77 K in gamma-ray irradiated ZnO single crystal. The bottom signal is a spectrum after successive illumination for 10 min with a red LED at 77 K.

Part of this research was presented at 34 th International Conference on Physics of Semiconductors (ICPS2018; Montpellier, France).

REFERENCES:

[1] Y. Torita, N. Nishikata, K. Kuriyama, K. Kushida, A. Kinomura, and Q. Xu, Proceedings of ICPS2016 (Journal of Physics, IOP(UK)) **864** (2017) 012016.

[2] T. Oga, Y. Izawa, K. Kuriyama, K. Kushida, and Q. Xu, Solid State Commun. **151** (2011) 1700.

[3] T. Kaida, K. Kamioka, T. Ida, K. Kuriyama, K. Kushida, and A. Kinomura, Nucl. Instrum, Method Phys. Res. B **332** (2014) 15.

[4] S. Lany and A. Zunger, Phys. Rev. B **72**, 165202 (2007).

[5] T. Oga, Y. Izawa, K. Kuriyama, K. Kushida, and A. Kinomura, J. Appl. Phys. **109** (2011) 123702.

[6] D. C. Look, J. W. Hemsky, and J. R. Sizelove, Phys. Rev. Lett. **82** (1999) 2552.

PR1-5 The first chalenging study on corrosion resistance of fusion divertor materials to liquid metal during electron irradiation

M. Akiyoshi, M. Kondo[1] and A. Kinomura[2]

Radiation Research Center, Osaka Prefecture University
[1]. Lab. for Nucl. Reactors, Tokyo Institute of Technology
[2]Inst. for Integrated Radiation and Nuclear Science, Kyoto University

INTRODUCTION:

Development of divertor material is one of the most important issues for future fusion reactor, where high thermal conductivity in severe neutron irradiation environment, sputtering resistance, and low radioactivity is required. Although development of SiC ceramics, tungsten, and its composite material is furthered, neither has resulted in the solution of this problem.

The liquid divertor is completely different approach from the conventional divertor material development, that is covering a surface of material with coolant liquid metal, and it can expect to moderate damage to the structure material. There is few study on the compatibility of liquid metal and structure material, and furthermore, compatibility study during irradiation is quite limited.

EXPERIMENTS and RESULTS:

Originally, it was planned to perform the corrosion experiment after an electron irradiation, however some corrosion on the surface cannot be prevented by underwater or in air irradiation. Therefore, in this study, tin (Sn) which is a candidate liquid metal coolant was sealed in a small irradiation container (30×34×4mm) created by SUS316L stainless steel, and performed electron irradiation by KURUNS-LINAC that achieved the corrosion action inner side of the container under irradiation environment.

In the irradiation container, aluminum rich ferritic steel (Fe-18Cr-3.3Al-0.4Si) NTK04L with 100μm Al_2O_3 oxidization coating was enclosed with tin, and the validity of ceramic coating under irradiation environment is verified.

In order to perform structure observation out side of the controlled area after the irradiation, irradiation energy was set to 8MeV, and other parameters were set as below; pulse frequency: 100Hz, pulse width: 4μsec, peak current: 250mA, and average current: 100μA. The irradiation experiment was performed during 2.4×10^5 s and achieved 1.1×10^{20} e on the irradiation container and the container was kept in the temperature range of 450 to 550 ℃ using air cooled copper heat sink.

After the irradiation, at the center of container, SUS316L plate had become thin, and a little leakage of tin was observed. It was scheduled to bring out the container for analyze immediately after the irradiation, however the container showed weak radioactivity of 560cpm with GM survey meter. Ge detector showed a transmutation nuclide of Sn-117 (half-life 13.6 days) is generated up to 10kBq. After the cooling period of more than two months, the surface dose showed background level that was checked by a radiological control technician.

In observation by an optical microscope on the cross-section, thinning of stainless container is observed, while Al_2O_3 coated NTK04L specimen showed no thinning. Further analysis is required to clarify the origin of this thinning, that is irradiation induced corrosion or concentration of beam heating or electro migration. Moreover, element distribution analysis by EPMA is advanced now.

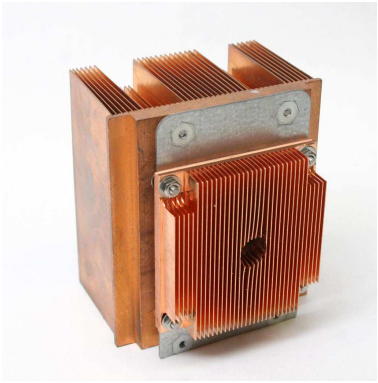

Fig.1 Cu heat sink used for the electron irradiation. The irradiation container was placed between two heat sinks. Pre heat sink was used as aperture (D 20mm).

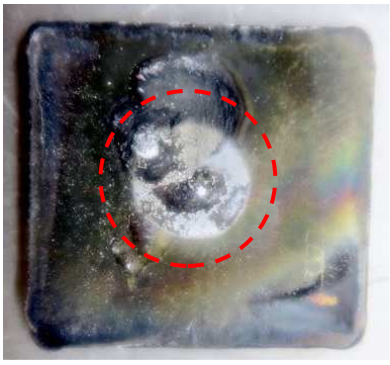

Fig. 2 Red circle shows small leakage of liquid tin from the stainless container. A thinning of the stainless plate was observed by cross-section observation.

PR1-6 Positron Annihilation Study of Fe-Cr binary alloy after Electron Irradiation

T. Onitsuka, K. Sato[1] and Q. Xu[2], J. Kinomura[2] and K. Fukumoto

Research Institute of Nuclear Engineering, Fukui University
[1]Graduate School of Science and Engineering, Kagoshima University
[2]Institute for Integrated Radiation and Nuclear Science, Kyoto University

INTRODUCTION: High-chromium (9-12%Cr) Ferritic/martensitic steels are attractive candidate material for various nuclear energy systems because of their excellent thermal properties, higher swelling resistance and lower activation compared with conventional austenitic stainless steels. The high-chromium steel as also been considered for both in-core and out-of-core applications of fast breeder reactors, and for the first wall and blanket structures of fusion systems, where irradiation induced degradation is expected to be the critical issues for reactor operation [1]. In the present study, the authors focused on a precipitation response for formation of α'-phase in Fe-Cr binary model alloy subjected to electron irradiation, in order to examine fundamental aspects of radiation effects on α'-phase precipitate development in iron-chromium alloys. The positron annihilation measurement technique was used to study the behaviour of microstructural evolution due to irradiation-induced defects and the formation of α'-phase simultaneously.

EXPERIMENTS: Simple binary Fe-40Cr alloy was made by arc melting under argon atmosphere in a water-cooled copper hearth. All the ingots were melted and inverted three times in order to promote chemical homogeneities. The obtained ingot was conducted by solution heat treatment at 1077 ℃ for 2 h followed by water quenching, and then, machined to the dimensions of 10 mm × 10 mm × 0.5 mm. The obtained specimen were irradiated by 9 MeV electrons at KURRI-LINAC. The specimen temperature was fixed at 100 or 475 ℃ during irradiation. The temperature variation was within ±5 ℃ during irradiation. The irradiation time was 88 hours for the batch of 100 ℃ irradiation test and varied from 1 to 10 hours for the batch of 475 ℃ irradiation tests. After the irradiation, all specimens were cooled immediately at the cooling rate of 170 ℃/min, and subsequently mechanically polished and electrolytically polished. Then, positron annihilation lifetime measurement and CDB measurement were performed.

RESULTS: Fig. 1. shows the positron annihilation lifetime measurement results of electron irradiated Fe-40Cr alloy. The longer lifetime components (τ_2) around 150 psec corresponds to vacancy type defects was obtained from a specimen irradiated at 100 ℃. On the other hand, the specimens irradiated at 475 ℃ show almost the same to bulk pure Fe. Fig. 2 shows the CDB ratio curves to bulk pure Cr obtained from positron CDB measurements for the Fe-40Cr alloy. The significant increase of the high-momentum fraction around 20 (P_L, 10^{-3}mc) observed for the specimens irradiated at 475 ℃. This behaviour suggests that the microstructural evolution of the annihilation fraction with electron of Fe due to the phase decomposition into Fe-rich (α) and Cr-rich (α') phases occurred in Fe-Cr alloy. Furthermore, the specimen irradiated at 100 ℃ showed almost similar behaviour in spite of the high concentration of defects.

REFERENCES:

[1] K. Okano *et al.*, Nucl. Instr. and Meth., **186** (1981) 115-120.

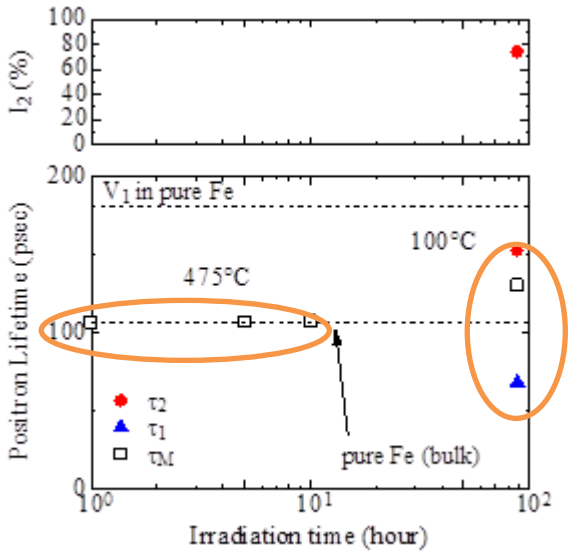

Fig. 1. The positron lifetime results with irradiation time for Fe-40Cr alloy. Bulk and a single vacancy (V_1) of pure Fe are also plotted as a reference.

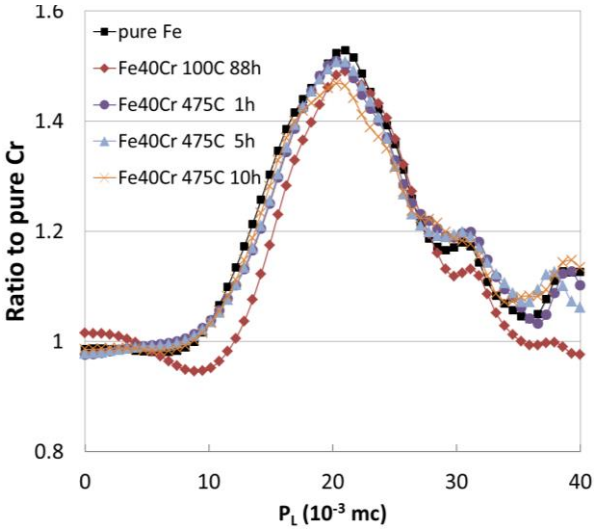

Fig. 2. The CDB ratio curves of irradiated specimens to unirradiated pure Cr. Unirradiated pure Fe is also plotted as a reference.

PR1-7 PAS Study on Free Volume in Several Diamond-like Carbon Thin Films

K. Kanda, F. Hori[1], A. Yabuuchi[2] and A. Kinomura[2]

Laboratory of Advanced Science and Technology for Industry, University of Hyogo
[1]Department of Materials Science, Osaka Prefecture University
[2]Institute for Integrated Radiation and Nuclear Science, Kyoto University

INTRODUCTION: The superlubricity of diamond-like carbon (DLC) film, along with its low friction coefficient, high hardness, chemical inert, and high wear and corrosion resistance, make it one of the most promising coatings for applications such as cutting tools, automobile parts, molds, computer hard disks, optical devices, food containers, and artificial blood vessels [1]. DLC film is amorphous carbon film that contains sp^3 hybridized carbon corresponding to a diamond structure and sp^2 hybridized carbon corresponding to a graphite structure. In addition, DLC film usually contains a certain amount of hydrogen [2].The chemical structure in terms of the coordination of carbon (sp^2 and sp^3 hybridization) and hydrogen atoms are the most important factors governing the quality of DLC films and they are used as classification criteria in ISO20523 published in 2017 [3]. However, DLC film also contains a certain amount of free volume. Free volume was considerable to connect strongly with several important properties of DLC film, such as hardness, Young modulus, and friction coefficient, but it has not been investigated. Positron annihilation spectroscopy (PAS) is a powerful tool for measuring free volume in material. In the present study, several DLC films were analyzed by PAS to evaluate the free volume in DLC films.

EXPERIMENTS: We worked on two kinds of experimental themes as for DLC films. One was the change of free volume in hydrogenated DLC film by the irradiation of soft X-ray. Sample was prepared by the hydrogenated DLC film exposed to synchrotron radiation (SR) at BL06 in the NewSUBARU synchrotron facility of the University of Hyogo [4]. The SR at the BL06 sample stage had a continuous spectrum from the infrared to soft X-ray region and an energy below 1 keV. Another theme was change of free volume by the doping of hetro-atom to DLC film. We deposited DLC films, which include and not include Si atoms, using PE-CVD method.

PAS measurement was performed at the slow positron beam system (B-1). Energy of incident positron, *E*, ranging 0.5 - 30 keV. Doppler broadening profiles of annihilation γ-rays were obtained using a Ge detector for each positron energy. The-low momentum part of spectra was characterized by the *S* parameter, which is defined as the number of annihilation events over the range of 511 ± 0.80 keV.

RESULTS: Figure 1 shows the *S* parameter as a function of incident positron energy *E* for the hydrogenated DLC films before and after irradiation of soft X-ray. The *S* values in the *E* region lower than 2 keV can be considered to attribute to the annihilation of positrons trapped in free volume in the DLC films. The *S* value of hydrogenated DLC film was lowered by the exposure to SR. This decrease was ascribable to the decrement of free volume in the hydrogenated DLC film by desorption of hydrogen from film due to excitation of soft X-rays [5].

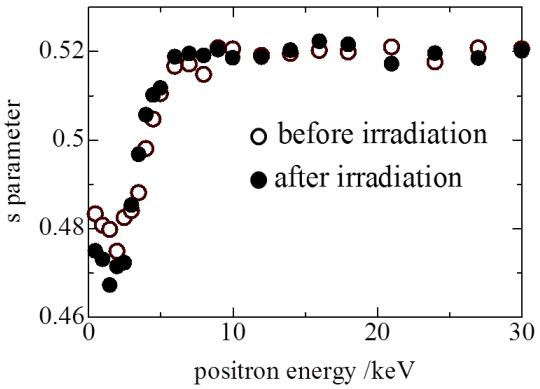

Fig. 1. *S* parameter as a function of positron energy *E* for hydrogenated DLC film before irradiation, ○ and that after irradiation of soft X-ray, ●.

Figure 2 shows the *S* parameter for the DLC films, which include and not include Si atoms. The *S* values of Si-containing DLC film were larger than those of DLC film which did not include Si. This result can be considered that Si atoms enhance the free volume in the DLC film.

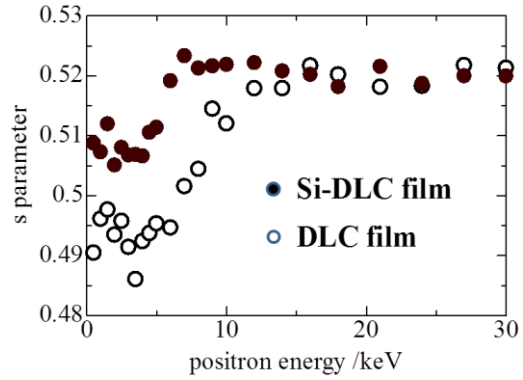

Fig. 2. *S* parameter as a function of positron energy E for DLC film, ○ and Si-DLC film, ●.

REFERENCES:

[1] S. Aisenberg *et al*., J. Appl. Phys. **42** (1971) 3963.
[2] J. Robertson, Surf. Coat. Technol. **50** (1992) 185.
[3] ISO20523, "Carbon based films – Classification and designations".
[4] K. Kanda *et al*., Jpn. J. Appl. Phys. **42** (2003) 3983.
[5] K. Kanda *et al*., Jpn. J. Appl. Phys. **50** (2011) 055801.

PR1-8 Positron annihilation spectroscopy on diamond-like carbon films

S. Nakao, X. Qu[1], A. Yabuuchi[1] and A. Kinomura[1]

Structure Materials Research Institute, National Institute of Advanced Industrial Science and Technology
[1]Institute for Integrated Radiation and Nuclear Science, Kyoto University

INTRODUCTION: Diamond-like carbon (DLC) films have attracted much attention because of their excellent mechanical properties, such as high hardness, high wear resistance and low friction coefficients. However, the properties strongly depend on the microstructure of the films which is varied by the deposition conditions and methods. Recently, DLC or carbon films are categorized from type I to VI, which includes graphite-like carbon (GLC) and polymer-like carbon (PLC).
The thermal stability of the films is of importance for practical applications. However, the thermal stability is not always enough to use it at high temperature. It is considered that the changes of the microstructure at high temperature should be responsible for the degradation of the properties. The structural changes are related to H desorption and behavior of defects at high temperature. Many studies have been carried out on the thermal stability of DLC films. However, the principal phenomena, such as defect behavior, are not always clear. Therefore, to make clear the thermal stability of DLC or carbon films, the examination on the defect behavior is necessary for every type of DLC films (type I to VI) because of different microstructure and hydrogen content. The positron annihilation spectroscopy (PAS) is one of the useful methods to clarify the defect behavior of materials. The aim of this project study is to examine the relationship between the thermal stability and the behavior of defects and bonded hydrogen in several types of DLC films by PAS and thermal desorption (TDS) method.
In a previous report [1,2], the films of type I, III, IV, V and VI were examined by TDS measurement in the range of room temperature (RT) to 800°C and it was found that hydrogen desorption clearly started around 400°C in the case of PLC (type VI) films. On the other hand, ta-C (type I) films did not change significantly until 800°C. It is well known that type I films are stable at high temperature. The result, thus, suggested that defects may be created by hydrogen desorption and the behavior may play important role for the durability of the films. In this study, several types of DLC and carbon films are examined by PAS measurement for the first attempt.

EXPERIMENTS: Samples for PAS measurement were type I, III – VI films. Type I (ta-C) and III (a-C) films were prepared by arc ion plating (AIP) at Nippon ITF Inc. and high-power impulse magnetron sputtering (HiPIMS), respectively. Type IV (a-C:H), V (GLC) and VI (PLC) films were deposited by plasma-based ion implantation (PBII) under the different conditions. The details on the PBII system were reported elsewhere [3]. Si wafer was used as substrate. The PAS spectra of Si substrate and graphite plate were also measured for comparison. The S-parameter was obtained at different positron energies ranging from 0 to 30 keV.

RESULTS: Figure 1 shows the change in S-parameter obtained from the PAS spectra of the samples at different positron energies in the range of 0 – 30 keV. The S-parameters of Si substrate and graphite plate are also indicated for comparison. In Fig. 1(a), the S-parameters of Si and graphite are around 0.51 and 0.47, respectively. On the other hand, the S-parameter of ta-C is a little bit lower than that of graphite, as shown in Fig.1(b). The other samples indicate similar S-parameter around 0.48. These results suggest that the situation of the defect in the type III – VI films may be similar in the case of as grown films. For the next stage, thermal annealing and PAS measurement is underway.

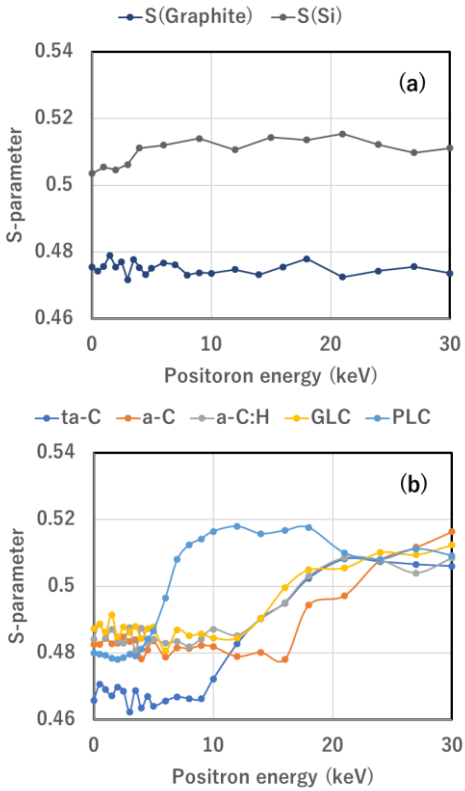

Fig.1. The change in S-parameter of the samples at different positron energies.

REFERENCES:

[1] S. Nakao *et al.*, KURRI Progress Report 2016, 28P12-8 (2016) 57.

[2] S. Nakao *et al.*, KURRI Progress Report 2017, 29P6-8 (2017) 32.

[3] S. Miyagawa *et al.*, Surf. Coat. Technol., **156** (2002) 322-327.